University of Texas Rio Grande Valley

ScholarWorks @ UTRGV

Mechanical Engineering Faculty Publications and Presentations

College of Engineering and Computer Science

3-1-2024

Characterization of Microstructural and Mechanical Properties of 17-4 PH Stainless Steel by Cold Rolled and Machining vs. DMLS Additive Manufacturing

Pablo Moreno-Garibaldi

Melvyn Alvarez-Vera

Juan Alfonso Beltrán-Fernández

Rafael Carrera-Espinoza

Héctor Manuel Hdz-García

See next page for additional authors

Follow this and additional works at: https://scholarworks.utrgv.edu/me_fac

 Part of the Mechanical Engineering Commons

Recommended Citation

Moreno-Garibaldi, Pablo, Melvyn Alvarez-Vera, Juan Alfonso Beltrán-Fernández, Rafael Carrera-Espinoza, Héctor Manuel Hdz-García, J. C. Díaz-Guillen, Rita Muñoz-Arroyo, Javier A. Ortega, and Paul Molenda. 2024. "Characterization of Microstructural and Mechanical Properties of 17-4 PH Stainless Steel by Cold Rolled and Machining vs. DMLS Additive Manufacturing" Journal of Manufacturing and Materials Processing 8, no. 2: 48. https://doi.org/10.3390/jmmp8020048

This Article is brought to you for free and open access by the College of Engineering and Computer Science at ScholarWorks @ UTRGV. It has been accepted for inclusion in Mechanical Engineering Faculty Publications and Presentations by an authorized administrator of ScholarWorks @ UTRGV. For more information, please contact justin.white@utrgv.edu, william.flores01@utrgv.edu.

Authors

Pablo Moreno-Garibaldi, Melvyn Alvarez-Vera, Juan Alfonso Beltrán-Fernández, Rafael Carrera-Espinoza, Héctor Manuel Hdz-García, J. C. Díaz-Guillen, Rita Muñoz-Arroyo, Javier A. Ortega, and Paul Molenda

This article is available at ScholarWorks @ UTRGV: https://scholarworks.utrgv.edu/me_fac/244

Journal of
Manufacturing and Materials Processing

MDPI

Article

Characterization of Microstructural and Mechanical Properties of 17-4 PH Stainless Steel by Cold Rolled and Machining vs. DMLS Additive Manufacturing

Pablo Moreno-Garibaldi [1], Melvyn Alvarez-Vera [1,*], Juan Alfonso Beltrán-Fernández [2], Rafael Carrera-Espinoza [1], Héctor Manuel Hdz-García [3], J. C. Díaz-Guillen [3], Rita Muñoz-Arroyo [4], Javier A. Ortega [5] and Paul Molenda [6]

1 Departamento de Ingeniería Industrial y Mecánica, Escuela de Ingeniería, Universidad de las Américas Puebla, Ex-Hacienda Santa Catarina Mártir S/N, Puebla 72810, Mexico; pablo.moreno@udlap.mx (P.M.-G.); rafael.carrera@udlap.mx (R.C.-E.)
2 Sección de Estudios de Posgrado e Investigación, Escuela Superior de Ingeniería Mecánica y Eléctrica, Unidad Profesional Adolfo López Mateos, Ciudad de México 07738, Mexico; jbeltran@ipn.mx
3 COMIMSA-Saltillo, Ciencia y Tecnología No. 790, Col. Saltillo 400, Saltillo 25290, Mexico; hmanuelhdz@comimsa.com (H.M.H.-G.); jcarlos@comimsa.com (J.C.D.-G.)
4 Facultad de Sistemas, Universidad Autónoma de Coahuila, Carr. A Mexíco Km. 13, Saltillo 25280, Mexico; munoz.r@uadec.edu.mx
5 Department of Mechanical Engineering, The University of Texas Rio Grande Valley, 1201 West University Drive, Edinburg, TX 78539, USA; javier.ortega@utrgv.edu
6 Engineering Department, Graduate School, Hof University of Applied Sciences, Alfons-Goppel-Platz 1, 95028 Hof, Germany; paul.molenda@hof-university.de
* Correspondence: melvyn.alvarez@udlap.mx

Abstract: The 17-4 PH stainless steel is widely used in the aerospace, petrochemical, chemical, food, and general metallurgical industries. The present study was conducted to analyze the mechanical properties of two types of 17-4 PH stainless steel—commercial cold-rolled and direct metal laser sintering (DMLS) manufactured. This study employed linear and nonlinear tensile FEM simulations, combined with various materials characterization techniques such as tensile testing and nanoindentation. Moreover, microstructural analysis was performed using metallographic techniques, optical microscopy, scanning electron microscopy (SEM) with energy dispersive spectroscopy (EDS), and X-ray diffraction (XRD). The results on the microstructure for 17-4 PH DMLS stainless steel reveal the layers of melting due to the laser process characterized by complex directional columnar structures parallel to the DMLS build direction. The mechanical properties obtained from the simple tension test decreased by 17% for the elastic modulus, 7.8% for the yield strength, and 7% for the ultimate strength for 17-4 PH DMLS compared with rolled 17-4 PH stainless steel. The FEM simulation using the experimental tension test data revealed that the 17-4 PH DMLS stainless steel experienced a decrease in the yield strength of ~8% and in the ultimate strength of ~11%. A reduction of the yield strength of the material was obtained as the grain size increased.

Keywords: additive manufacturing (DMLS); machining manufacturing; 17-4 PH stainless steel; mechanical properties; finite element method; elastic modulus

check for updates

Citation: Moreno-Garibaldi, P.; Alvarez-Vera, M.; Beltrán-Fernández, J.A.; Carrera-Espinoza, R.; Hdz-García, H.M.; Díaz-Guillen, J.C.; Muñoz-Arroyo, R.; Ortega, J.A.; Molenda, P. Characterization of Microstructural and Mechanical Properties of 17-4 PH Stainless Steel by Cold Rolled and Machining vs. DMLS Additive Manufacturing. *J. Manuf. Mater. Process.* **2024**, *8*, 48. https://doi.org/10.3390/jmmp8020048

Academic Editors: Hamed Asgari and Elham Mirkoohi

Received: 24 January 2024
Revised: 17 February 2024
Accepted: 22 February 2024
Published: 1 March 2024

Copyright: © 2024 by the authors. Licensee MDPI, Basel, Switzerland. This article is an open access article distributed under the terms and conditions of the Creative Commons Attribution (CC BY) license (https://creativecommons.org/licenses/by/4.0/).

1. Introduction

The present research focuses on the precipitation-hardened martensitic stainless steel 17-4 PH, a material well known for its applications in aviation [1], automotive [2], medical [3], tooling [4], marine [5], nuclear, military, food, and petroleum sectors [6–8], due to its good resistance to high temperature, fracture, oxidation, and corrosion, the main objective being to find the differences in the mechanical and microstructural properties of this material manufactured via cold rolling and DMLS.

It is well known that the mechanical properties of the materials change depending on the method of its manufacture, such as conventional manufacturing processes (stamping, rolling, forging, etc.) or additive manufacturing processes, which is why some studies have been carried out regarding the differences in the mechanical properties of different materials under different manufacturing processes, finding differences in tensile strengths, Young's modulus, fatigue limits, ductility, etc. [9,10]. For example, Luecke performed a study that demonstrated that the tensile mechanical properties of the 17-4 PH SS fabricated by selective laser melting are very different from those of wrought steel [11], the differences being in the microstructure, something crucial for the performance of the material. These findings were supported by Yeon, because he found that laser powder bed fusion (L-PBF)-processed 17-4 PH stainless steel generally exhibits a non-equilibrium microstructure consisting mostly of columnar δ-ferrite grains and a substantial fraction of retained austenite and martensite, contrary to 17-4 PH SS wrought with a fully martensite structure and coarse grains [12]. Another study made a comparison of the tribological behavior of 17-4 PH SS manufactured via conventional and additive manufacturing methods, and the results showed that AM parts have good potential to be an alternative to counterparts in terms of friction and wear behavior [13]. To summarize, processing conditions can affect the final metallurgical, mechanical, and geometrical properties of the material [14].

Analyzing the conventional processes separately, one of the most common is called the rolling process, commonly used to produce different shapes such as bars [15], pipes [16], sheets [17], and strips [18]. In the rolling process, an input feed of metal is forced to pass through two specially designed rollers, which roll in opposite directions [19], obtaining different shapes depending on whether it is applied to cold or hot rolled techniques. Cold rolling is usually applied during the processing of austenitic stainless steel, which can be used for strengthening, work-hardening, and grain refinement during annealing. This method impacts microstructure, phase transformation, and mechanical properties [20]. For all these reasons, rolling techniques in metal forming operations have been widely studied to analyze the defects and potential application areas for products and components [21].

On the other hand, since the emergence of additive manufacturing technologies, barriers to design have been removed, and the way products are manufactured has changed dramatically [22]. Additive manufacturing (AM) operates on the principle of constructing a three-dimensional model layer by layer, facilitated by computer-aided design (CAD) software [23]. In the realm of metal printing technologies, prominent examples include laser metal fusion (LMF), selective laser melting (SLM), and direct metal laser sintering (DMLS) [24,25]. These methodologies have undergone extensive investigation to elucidate their impact on material performance, considering factors such as porosity [26], process parameters, building atmosphere, post-heat treatments, and initial powder characteristics. These investigations have focused on phase transformation, microcrack formation, microstructure evolution, and mechanical properties, particularly in stainless steel materials [27–29]. Additionally, comparative studies have been undertaken regarding similar AM technologies. For example, a comparison made by Nezhadfar regarding 17-4 PH manufactured via laser powder bed fusion (L-PBF) and laser powder directed energy deposition showed that the L-PBF specimens have a finer microstructure (ferrite + lath martensite) than the LP-DED ones (massive ferrite + Widmanstätten ferrite) in non-heat treated conditions [30]. Another example was performed by Akessa in which the mechanical properties of 17-4 PH manufactured via Markforged metal X (MfMX) describe a lower tensile strength but a similar hardness compared with others fabricated via laser powder bed fusion [31].

Due to several factors that can modify or influence the mechanical properties of the stainless steels manufactured via AM technologies, such as powder chemistry, processing environment, grain diameter, etc. [32], it is essential to provide more details of the most important ones:

1. Printing orientation: Cases where 316 SS was printed via atomic diffusion additive manufacturing (ADAM) in the direction of loading showed strength and strain to failure improvement of greater than 10% compared with other orientations [33]. Printed spec-

imens of 17-4 PH and 316 SS in different orientations and using selective laser melting (SLM) showed a noticeable effect on tensile properties [34,35]. The same happens with other studies related to the same material where the best tensile properties are shown on specimens printed in a flat layout compared with the vertical layout [36–38], results reinforced by the research carried out by Alkindi, where the specimens were printed from 0° until 90° increasing 10° by each other obtaining the same results [39].

2. Heat treatment: The study carried out by Malakshah analyzes the effect of heat treatment on the mechanical behavior of 17-4 PH and demonstrates that corrosion resistance and fatigue resistance were superior [40], results that are supported by Nezhadfar finding that fatigue strength is improved considerably [41]. Meanwhile, Huber improved the ultimate tensile strength (UTS), the elongation break, and the hardness with the influence of sintering temperature and hold time on densification [42]. Another study performed by Wilcox involved the same material being treated at different temperatures to give a wide range of mechanical properties [43].

3. Particle size: Feng demonstrates that the characteristics of the raw metal powder affect the microstructure and performance of the 17-4 PH processed by SLM [44], results supported by other authors using different metal powders with different chemical compositions and particle sizes, obtaining different properties related to hardness, elongation, and UTS [45,46].

4. Process environment during AM processes: Sandy demonstrates that the presence of oxide layers in stainless steel manufactured via AM technologies was correlated with the interaction of atmospheric oxygen with the chromium present in these materials [47].

5. Chemical composition, laser power, and scan speed: The study carried out by Sarma indicates that the variation in chemical composition is reflected in variations in relative density and microhardness. In addition, the same investigation found that changes in laser power and scan speed in the printing process impact the density and microhardness of the 17-4 PH SS [48].

The main advantages of AM are that this technology produces near net shapes in less time compared to conventional manufacturing processes [49]. Also, this technology can fabricate parts with extremely complicated structures that cannot be fabricated by traditional methods [50]. However, there are some disadvantages like porosity, remelting, solidification, and rapid melting of the powder during the production of parts, and a complex microstructure [50]. Moreover, the mechanical properties of AM such as yield strength, ultimate tensile strength, and elongation at fracture are influenced by the microstructure [51]. In addition, due to the complexity of AM structures and variables involved in the mechanical behavior of materials, it can be simulated using experimental data, extracting properties from the experimental tests and using this information as input for numerical models to obtain accurate mechanical properties predictions [52,53]. This study aims to evaluate the impact on the mechanical properties and microstructure of 17-4 PH stainless steel specimens produced through two different manufacturing processes: traditional machining from commercial cold rolled 17-4 PH stainless steel and direct metal laser sintering DMLS 17-4 PH stainless steel. The mechanical properties evaluation is conducted through experimental tensile testing and nanoindentation analysis. The experimental results were used to generate the materials database for finite element simulations, which will be useful for predicting the mechanical behavior of structures produced by different manufacturing processes.

2. Materials and Methods

Experimental Procedure

In this study, 17-4 PH stainless steel specimens were produced using two different manufacturing processes: traditional machining from commercial cold rolled 17-4 PH and direct metal laser sintering (DMLS). The schematic of the metal removal machining process and direct metal laser sintering (DMLS) are shown in Figure 1. To manufacture the tensile test samples with the metal removal machining process, commercial circular cold rolled

17-4 PH with 30 mm diameter and 100 mm length was sectioned and machined using the conventional metal removal process. The parameters used for the removal process involved cutting velocity, feed per revolution, and cutting depth, which were 80 m/min, 0.02 mm/r, and 0.5 mm, respectively. The DMLS tensile specimens were also manufactured with an EOS M 300-4 series printer with DMLS technology, as shown in Figure 1. The selected DMLS parameters of laser beam diameter, power, and scanning speed were 0.1 mm, 400 W, and 7 m/s, respectively. The small-size samples were selected according to ASTM A370-03a [54], as shown in Figure 2.

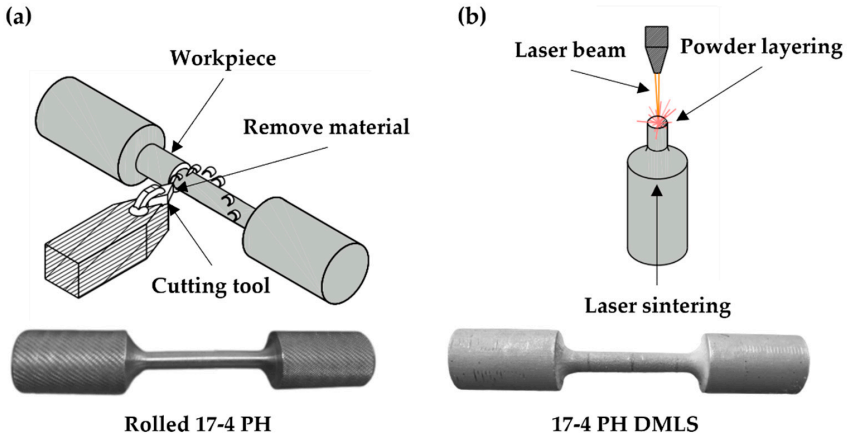

Figure 1. Manufacture processes for tensile samples: (**a**) metal removal process and (**b**) direct metal laser sintering (DMLS).

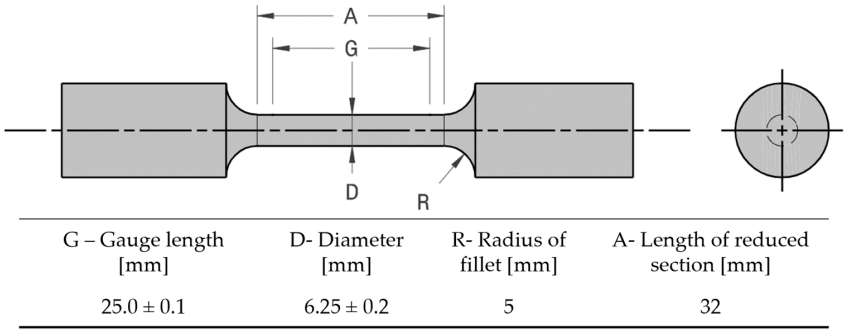

Figure 2. Small-size specimens proportional to standard ASTM A370-03a.

The materials used for the present study were commercially rolled 17-4 PH (ARMCO®® AK steel International, Cologne, Germany 17-4 PH®® Stainless steel) and DMLS 17-PH stainless steel (EO5 Stainless steel 17-4 PH powder). The chemical composition of commercially rolled 17-4 PH and 17-4 PH stainless steel manufactured by DMLS (EOS StainlessSteel, Munich, Germany) is presented in Table 1.

Table 1. Chemical composition wt. % of 17-4 PH and 17-4 PH DMLS stainless steel.

Element	Cr	Ni	Cu	Mn	Nb	C	Si	Fe
Rolled 17-4 PH	15–17.5	3–5	3–5	1	0.15–0.45	0.07	1	Bal.
17-4 PH DMLS	15–17.5	3–5	3–5	1	0.15–0.45	0.07	1	Bal.

Two tensile test samples of rolled 17-4 PH and 17-4 PH (DMLS) were analyzed for microstructure. Prior to the test, the samples were cut on the cross-section in both longitudinal and transversal directions. They were then mounted and polished using a conventional metallographic polishing procedure. An electrolytic process involving a solution containing 10 mL of H_3PO_4, 40 mL of HNO_3, and 50 mL of H_2SO_4 was used to etch the

samples. The voltage was set at 3 V and the current at 3.5 A for 3 s. The cross-section of longitudinal and transversal sections of rolled 17-4 PH and 17-4 PH (DMLS) substrate melted area were observed under an optical microscope. Scanning electron microscopy (SEM, Tescan Mira 3(TESCAN GROUP, a.s., Kohoutovice, Czech Republic)) with energy dispersive X-ray spectroscopy (EDS, Bruker (Bruker, Hamburg, Germany)) was used to evaluate the microstructure and semi-quantitative chemical composition of the samples. The crystalline phases were determined by an X-ray diffraction analysis (XRD, Phillips X'Pert 3040, Bragg-Brentano (PANALITICAL, Great Malvern, UK) over a 2-theta range from 40 to 90 degrees by using Cu-Kα radiation at 25 kV–30 mA.

The mechanical properties were experimentally assessed using a tensile test which was performed three times for each condition of rolled 17-4 PH and 17-4 PH stainless steel manufactured by direct metal laser sintering (DMLS) using an INSTRON model 8502 (INSTRON, Norwood, MA, USA) universal testing machine at a rate of 5 mm/min test speed. During the tensile test for both conditions, the elongation was recorded with an extensometer by using a gauge length. The microhardness and elastic modulus were determined via nanoindentation tests using an RTec Instrument with a 300 mN load and a 12 s hold time.

3. Simulation Configuration

Numerical Simulation by Finite Element Method

The 3D CAD model dimensions of the tensile test samples were used according to standard ASTM A370-03a for rolled 17-4 PH and 17-4 PH stainless steel manufactured by direct metal laser sintering (DMLS). The numerical simulation tensile test was performed using the commercial SolidWorks®® software 2022. Numerical tensile test simulations using the finite element method were performed using linear and advanced nonlinear simulations with dynamic analysis. The meshes of rolled 17-4 PH and 17-4 PH DMLS were created using a fine mesh with a curvature-based mesh with a minimum and maximum element size of 1.2 mm (average size), resulting in 57,353 tetrahedral elements and 83,819 nodes (as shown in Figure 3). A mesh independence analysis was performed, decreasing five different element sizes from medium to fine, being from 2.5 mm to 1.2 mm, to determine the converged solution to optimize the computational time. The mechanical properties of elastic modulus, Poisson´s ratio, tensile strength, and yield strength of materials were determined by experimental tensile tests, and data using the average experimental stress–strain curves were set in the simulation model type of plasticity–von Mises to create the stress–strain curves available in SolidWorks®® software 2022. The boundary conditions for the samples were set on one side, and were totally fixtured. Meanwhile, the constraint for the other side was a cylindrical axial translation according to the experimental maximum lengths of 5.2 mm and 4.2 mm for rolled 17-4 PH and 17-4 PH stainless steel manufactured by direct metal laser sintering (DMLS), respectively. The stress analysis for the tensile test samples under translation conditions was considered using the experimental tensile velocity of 2.5 mm/min.

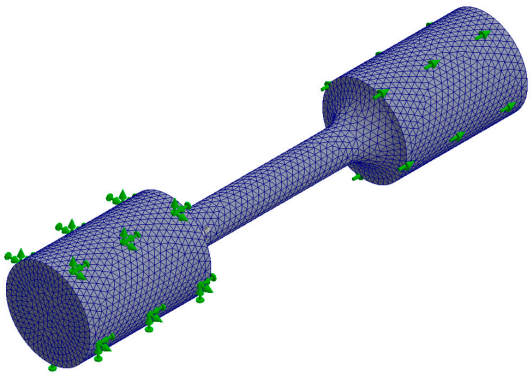

Figure 3. Mesh, constraint, and translation conditions for rolled 17-4 PH and 17-4 PH DMLS.

4. Results and Discussion

4.1. Microstructural Characterization

The microstructure at low magnifications for the rolled 17-4 PH and 17-4 PH stainless steel obtained longitudinal and transversal cross-sections of tensile samples, which are shown in Figure 4. The micrographs in Figure 4a show the microstructure of the rolled 17-4 PH stainless steel with the presence of a typical martensitic structure. The cross-section microstructure in longitudinal and transversal regions showed a fine crystalline martensitic microstructure. The comparison of the cross-section micrographs shows that the microstructure that appeared in both areas is the same. The micrographs of Figure 4b reveal the layers or levels of melting of the steel powder due to the laser. These layers have a thickness of 70 μm; this is seen in the longitudinal section of the figure, while the transversal section, with a lower magnification, shows the elongated shapes of microstructure on the material in the transversal direction manufactured by the DMLS process.

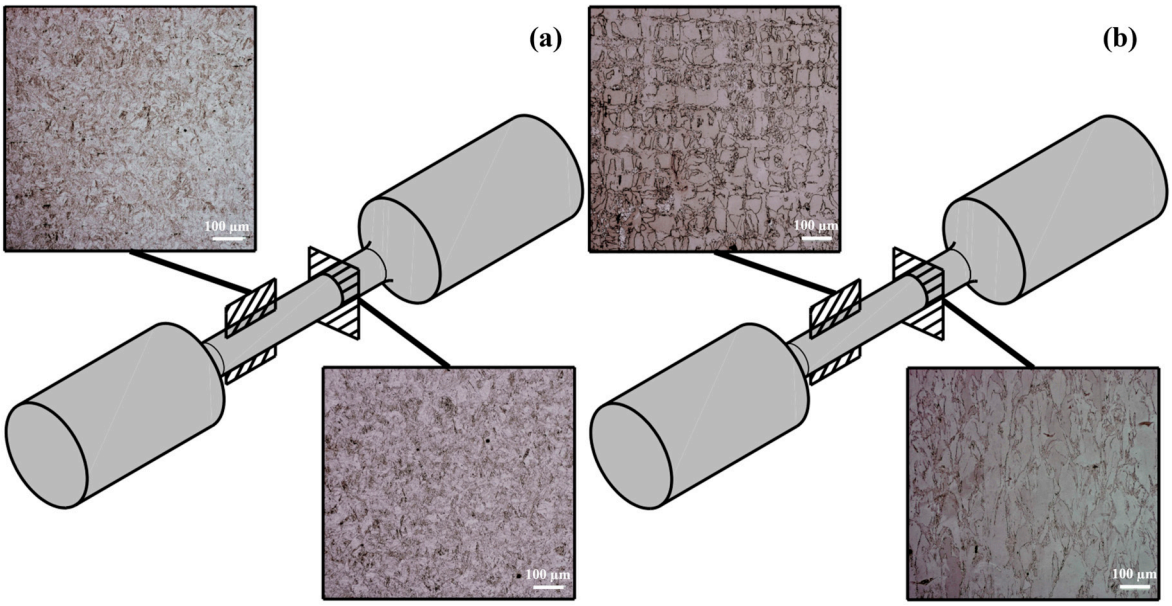

Figure 4. Optical micrographs of cross-sections for longitudinal and transverse planes for (**a**) rolled 17-4 PH and (**b**) 17-4 PH DMLS.

SEM micrographs of the microstructure at high magnifications and EDS semi-quantitative chemical compositions for the rolled 17-4 PH and 17-4 PH DMLS stainless steel obtained longitudinal and transversal cross-sections of tensile samples, which are shown in Figure 5. The micrographs of Figure 5a,b show the longitudinal and transversal microstructures for the rolled 17-4 PH stainless steel and a typical martensitic structure. The EDS and semi-quantitative chemical composition show the chemical elements for 17-4 PH stainless steel. The 17-4 PH DMLS stainless steel microstructure is characterized by complex directional columnar structures parallel to the DMLS build direction shown in Figure 5c. According to the microstructures presented in optical and SEM micrographs shown in Figures 4 and 5, respectively, the difference in grain morphology and size distribution can be seen, showing for the rolled 17-4 PH a small grain compared with those obtained by the DMLS process, impacting the mechanical properties of the materials analyzed. According to Porro et al. [51], who analyzed the Hall–Petch effect, it shows a correlation between yield strength and grain size, describing a reduction of the yield strength of the material as the grain size increases. This effect is supported by the results obtained, having a rolled small grain of 358.9 μm^2 (767 ± 6.4 MPa) and for DMLS a large grain of 2539.6 μm^2 (707 ± 13.3 MPa).

Diffraction XRD patterns for both rolled 17-4 PH and 17-4 PH DMLS stainless steel samples were analyzed for the cross-sections in longitudinal and transversal directions, as shown in Figure 6a and Figure 6b, respectively. The diffraction of rolled 17-4 PH stainless

steel presents an austenitic (γ) phase (ICDD:04-020-7293) ((111) at 43.57°, (200) at 51.11°, (220) at 75.19°), and a ferritic (α) phase (ICDD:04-011-9042) ((110) at 44.68°, (200) at 65.03°, (211) at 82.34°)), shown in Figure 6a. The XRD patterns of 17-4 PH DMLS stainless steel show the presence of both ferritic alpha (α) or martensitic phase (Ref. code: 00-044-1290) ((101) at 44.18°, (110) at 44.80°, (200) at 65.22°, (211) at 82.16°), and austenitic (γ) phase. Based on the diffraction patterns, the microstructure contains both ferritic and martensitic microstructures in the 17-4 PH DMLS stainless steel, as does austenitic gamma microstructure, shown in Figure 6b. These results agree with other authors' observations [55,56].

4.2. Experimental Characterization of Mechanical Properties

The mechanical properties of steel under different manufacturing methods are important due to the change in their behavior and mechanical strength. For this case study, after analyzing the data obtained by the tensile testing machine, the stress–strain graph was obtained for the materials bar of 17-4 PH and 17-4 PH DMLS stainless steel (see Figure 7a,b). The parameters obtained from the simple tension test are the yield stress, obtained through a linear regression of the linear–elastic zone, and the method is applied at 0.2% of the unit strain. The ultimate stress is found in the plastic deformation zone, which reaches the maximum stress. Finally, the elastic modulus is determined by the slope in the linear–elastic region. The numerical values of the mechanical properties of elastic modulus, yield stress, ultimate stress, and HRC hardness of the materials are shown in Table 2 of the steel tensile and hardness test results.

Table 2. Mechanical properties determined by tensile test of rolled 17-4 PH and 17-4 PH DMLS stainless steel.

Property	Rolled 17-4 PH	17-4 PH DMLS
Elastic modulus (E) GPa	200 ± 1.8	166 ± 4.1
Yield strength YS (σ_y) MPa	767 ± 6.4	707 ± 13.3
Ultimate strength UTS (σ_μ) MPa	965 ± 9.2	897 ± 22.9
Elongation %	21.2 ± 0.7	16.8 ± 0.4
Hardness ($HV_{0.1}$)	298 ± 3.8	312 ± 8.76

The stress–strain for both processing methods was defined in the linear elastic behavior with the engineering stress using Equation (1):

$$\sigma = \left(\frac{F}{A_0}\right), \tag{1}$$

and the strain using Equation (2):

$$\epsilon = \left(\frac{\delta}{L_0}\right) \tag{2}$$

was determined to calculate the mechanical properties shown in Table 2. The parameters were taken from the corresponding experimental stress–strain curves shown in Figure 7.

When making a comparison between both the processing methods analyzed, some differences can be observed regarding the strength of the material, information that is presented in Table 2. The results show a reduction of rigidity of 17% in the material manufactured via DMLS compared with that manufactured by rolling and, after researching the mechanical properties of SS materials with different manufacturing methods, it was observed that variations in the mechanical properties could be focused more on the material processed with AM technologies; different factors could be the reason for this, such as chemical composition, the AM technology used for the manufacturing process, printing parameters, powder particle size, etc. For example, the lowest rigidity was reported by Suwanpreecha with 159 GPa [36], while Henry found 176 GPa [33], and a maximum value of 206.7 GPa was reported by Carneiro [9]. On the other hand, for the case of the

rolled material, a similar value was reported by Carneiro (200 GPa) [9], compared with the 200 ± 1.8 GPa stated in the present research.

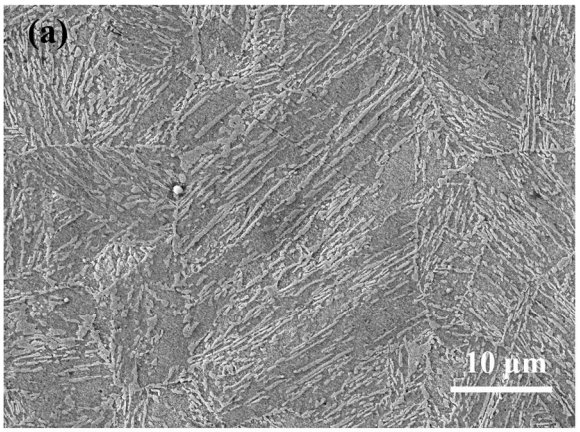

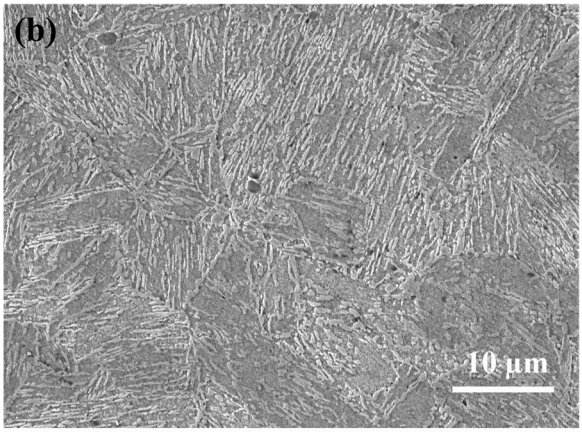

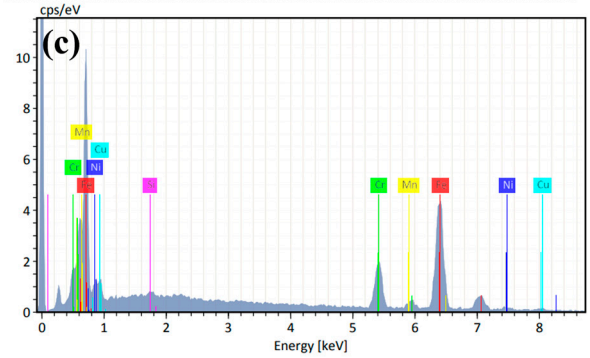

Element	Mass Norm. [%]	Atom [%]
Iron	74.91	74.41
Chromium	15.59	16.63
Nickel	3.27	3.09
Copper	5.19	4.53
Silicon	0.31	0.61
Manganese	0.73	0.73

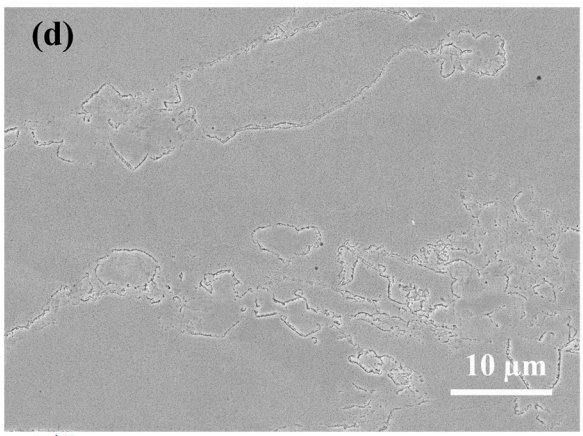

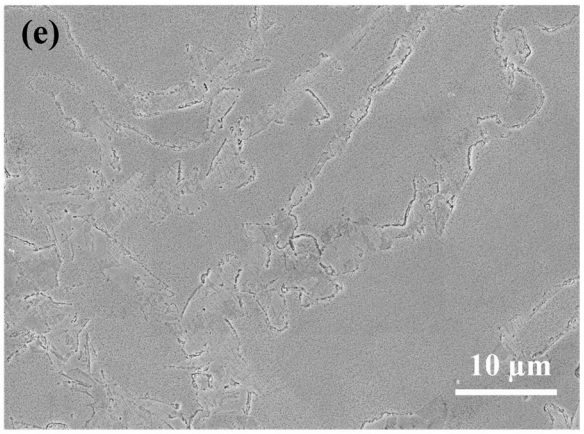

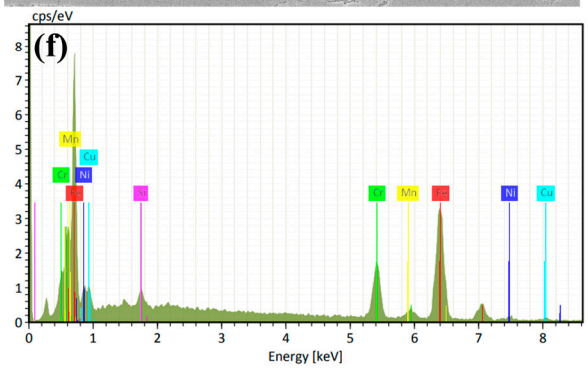

Element	Mass Norm. [%]	Atom [%]
Iron	71.75	70.77
Chromium	16.89	17.95
Nickel	4.62	4.35
Copper	5.85	5.09
Silicon	0.32	1.52
Manganese	0.57	0.32

Figure 5. SEM and EDS with semi-quantitative analysis for rolled 17-4 PH: (**a**) longitudinal, (**b**) transversal, and (**c**) EDS and for 17-4 PH DMLS: (**d**) longitudinal, (**e**) transversal, and (**f**) EDS.

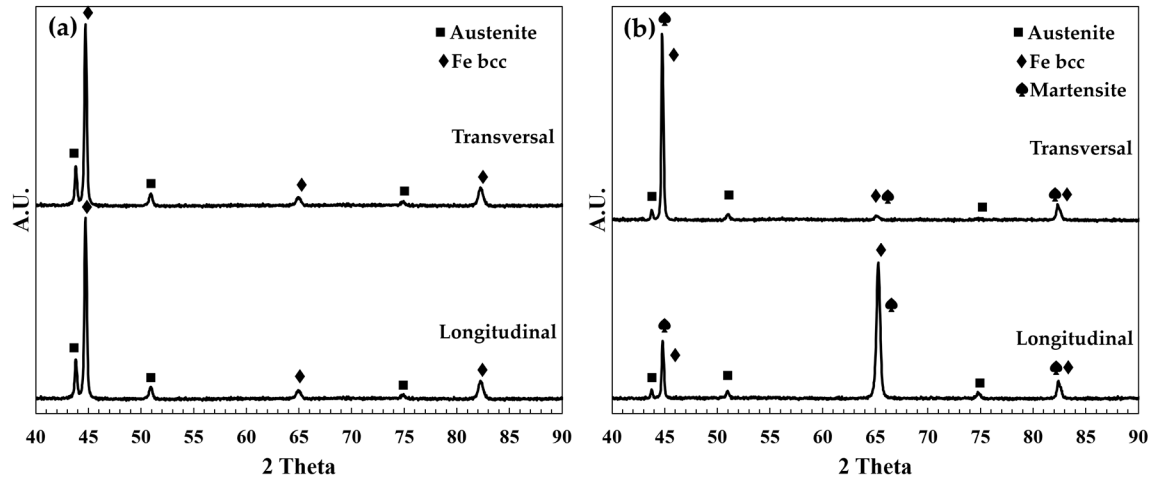

Figure 6. Diffraction XRD patterns for (**a**) rolled 17-4 PH and (**b**) 17-4 PH DMLS.

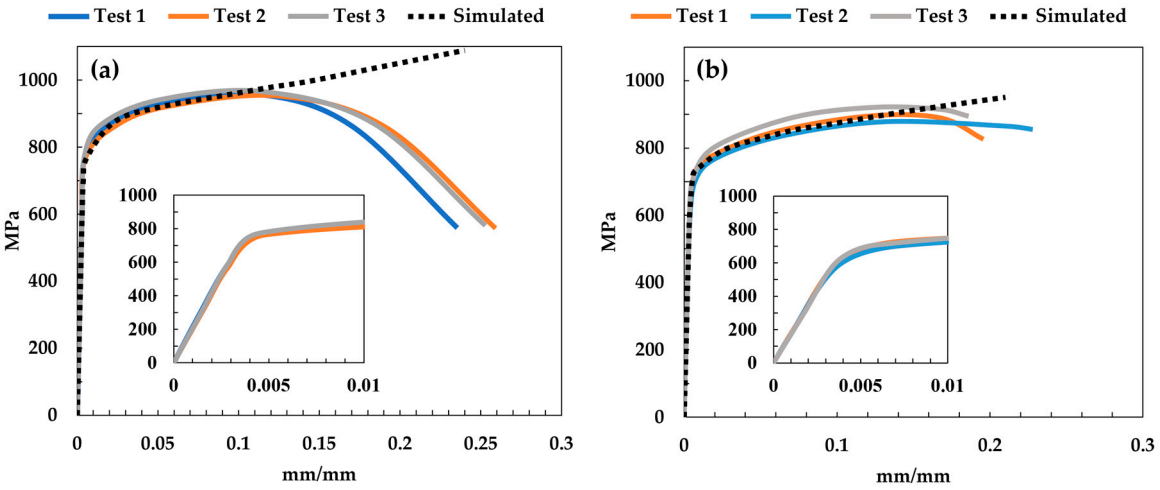

Figure 7. Stress–strain experimental and FEM simulated curves for (**a**) rolled 17-4 PH and (**b**) 17-4 PH DMLS.

Other parameters to take into consideration are the yield stress and UTS. The values reported in the present investigation for the AM material are 707 ± 13.3 MPa and 897 ± 22.9 MPa, respectively, while others report similar values. For example, Henry found values of 600 MPa for yield stress and 800 MPa for UTS [33]; then Suwanpreecha reported 668 ± 40 MPa for yield stress and 745 ± 6 MPa for UTS [36], and other studies report higher mechanical properties, for example, Sghaier found 992 MPa for yield stress and 1018 MPa for UTS. Still, the material faced a post-processing treatment [27].

The hardness value obtained was 298 ± 3.8 HV for rolled and 312 ± 8.76 HV for AM, similar to those obtained by other authors. For example, Gatoes mentions a range of 250–460 HV for rolled and 306 ± 11 HV for AM [28], while Akessa reports a hardness of 331 ± 28 HV for AM material [31].

The mechanical properties with nanoindentation for rolled 17-4 PH and 17-4 PH DMLS stainless steel samples were measured with three nanoindentation curves in the cross-sections in longitudinal and transversal directions, as shown in Figure 8. The curves of rolled 17-4 PH and 17-4 PH DMLS stainless steel for longitudinal and transversal directions are shown in Figure 8a,b and Figure 8c,d, respectively. The values of maximum depth for rolled 17-4 PH ranged from 2036 up to 2074 μm for the longitudinal and from 2033 up to 2083 μm for the transversal section, which is indicative of higher deformation compared with 17-4 PH DMLS, as shown in Figure 8a,b. The depth values for rolled 17-4

PH DMLS ranged from 2046 to 2178 µm for the longitudinal and from 1876 to 1934 µm for the transversal section, as shown in Figure 8c,d. On the other hand, as detailed in Figure 8a–d, the presence of the "nose" during unloading is evidence of the mechanical behavior of the indented material, which depends on the time [57,58]. This phenomenon can be interpreted as a recovery (elastic or plastic) during unloading under the conditions of the tests. Comparatively, the 17-4 PH DMLS sample displays a slight elastic deformation in the transversal direction compared to the longitudinal direction. Meanwhile, the "nose" is more marked in both directions of the 17-4 PH samples as well as in the longitudinal direction of the 17-4 PH sample, which indicates slight plastic deformation. In this case, as suggested in the literature [57–59], another way to evaluate or confirm this mechanical behavior is to calculate the coefficient of elastic recovery parameter (k_e) using the equation that describes the effect of the maximum load on elastic/plastic deformation. In this case, the k_e parameter reflects the elastic recovery of the material during the unloading process. Therefore, k_e can be calculated from the data extracted from the curve obtained by applying the nanoindentation technique and using Equation (3):

$$k_e = \left(1 - \frac{h_f}{h_{max}}\right) \times 100, \quad (3)$$

where k_e (%) is the coefficient of elastic recovery, h_{max} (µm) is the maximum penetration depth, and h_f (µm) is the residual depth after unloading.

In this sense, Table 3 presents the values of the elastic recovery parameter of both samples. It is shown in detail that the 17-4 PH DMLS sample in the transversal direction has a higher value of elastic recovery of ~28.50% than in the longitudinal direction. By contrast, the 17-4 PH sample has values of ~22.38% in the longitudinal direction and 22.23% in the transversal direction, which establish a less elastic recovery parameter. Likewise, the average maximum indentation depth, elastic modulus E, nanohardness H, contact stiffness S, and elastic recovery parameter (k_e) are summarized in Table 3. It is possible to observe a difference in elastic modulus E, which results in longitudinal and transversal directions for 17-4 PH DMLS due to the superposition of the DMLS layers. Alfieri et al. have discussed this anisotropic behavior in terms of the influence of building direction [60].

Table 3. Mechanical properties by nanoindentation at 300 mN.

Sample	Depth (nm)	*E* (GPa)	*H* (GPa)	S (N/m)	K_e (%)
Rolled 17-4 PH-L	2056 ± 18.87	187 ± 14.8	2.93 ± 0.09	147.3 ± 2.2	22.38 ± 28.30
Rolled 17-4 PH-T	2083 ± 21.79	189 ± 12.4	2.91 ± 0.13	145.9 ± 1.7	22.23 ± 29.62
17-4 PH DMLS-L	2128 ± 21.79	144 ± 16.1	2.84 ± 0.26	142.5 ± 5.1	25.08 ± 30.56
17-4 PH DMLS-T	1901 ± 29.56	171 ± 13.3	3.01 ± 0.13	159.8 ± 2.2	28.50 ± 38.5

The simulations of linear tensile test results for rolled 17-4 PH and 17-4 PH DMLS were performed to evaluate the transient evolution of von Mises stress and axial displacement at yield strength as shown in Figure 9a. The ultimate strength and fracture strength for rolled 17-4 PH and 17-4 PH DMLS stainless steel samples were nonlinearly simulated using the plasticity–von Mises model for multi-linear stress–strain curve definition, where the stress–strain curves were experimentally obtained, as shown in Figure 9b and Figure 9c, respectively.

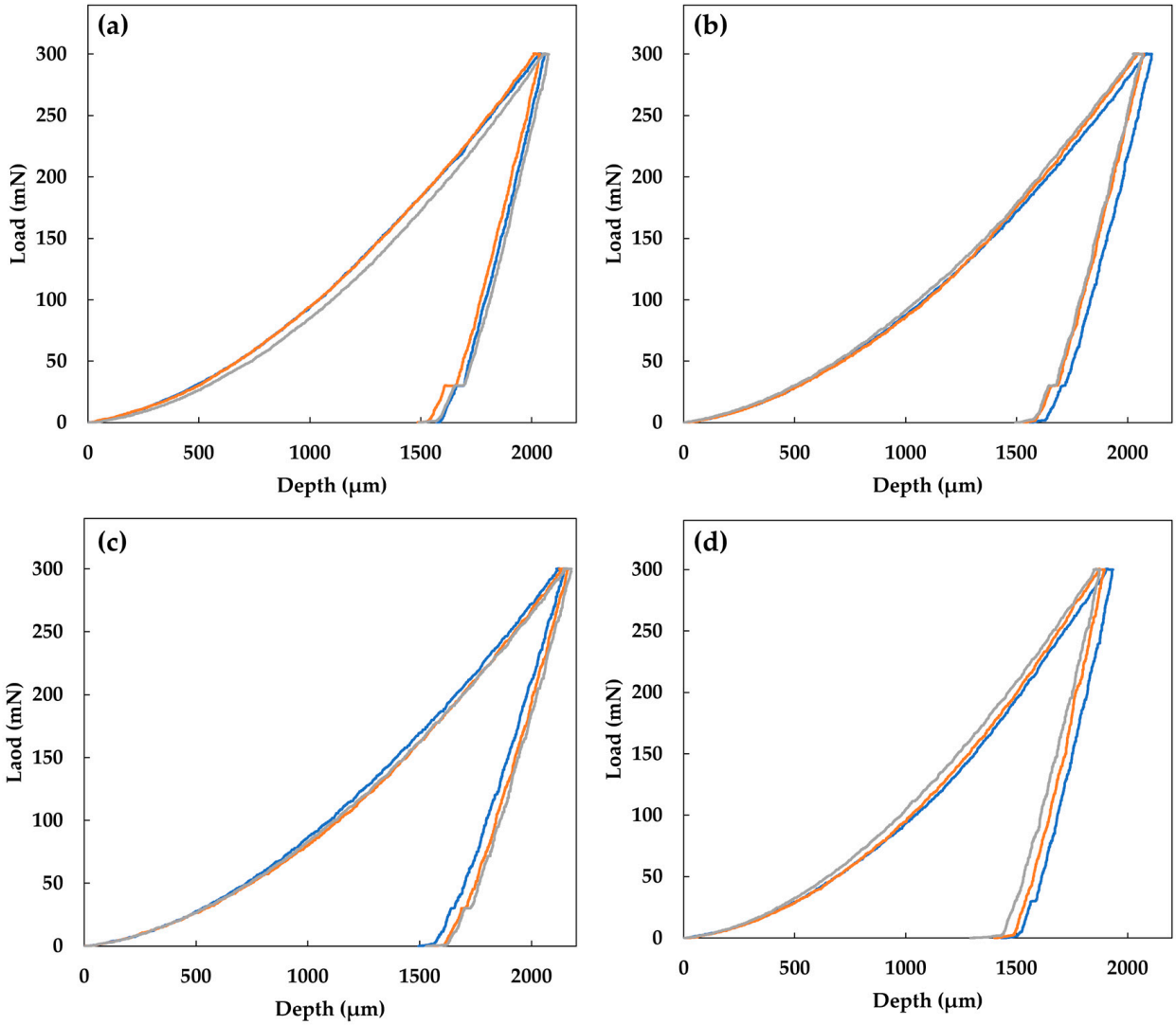

Figure 8. Nanoindentation experimental load–unload curves of the cross-section for rolled 17-4 PH: (**a**) longitudinal, (**b**) transversal, and for 17-4 PH DMLS: (**c**) longitudinal, (**d**) transversal. The three colors (blue, gray and orange) represent the results of three nanoindentation repetitions for each test condition.

The von Mises stress and axial displacement at yield strength were 770.04 MPa and 0.13 mm (Figure 9a). These values correspond to the maximum linear behavior according to Hooke's law. After this, the nonlinear behavior is reached in the strain-hardening with 983.9 MPa and 2.795 mm (Figure 9b). Finally, the necking region is obtained until fracture strength reaches 1116 MPa and 5.5 mm (Figure 9c). In the same way, DMLS stainless steel was evaluated in the linear and nonlinear regions for yield strength, ultimate strength, and fracture strength, as shown in Figure 10a, Figure 10b and Figure 10c, respectively. The von Mises stress and axial displacement at yield strength were 708.2 MPa and 0.156 mm in the linear behavior, as shown in Figure 10a. After this point, the nonlinear behavior is reached in the strain-hardening with 871.5 MPa and 2.08 mm, as shown in Figure 10b. The necking region and fracture strength are reached with 957.2 MPa and 4.2 mm (Figure 10c). According to the experimental and simulated and experimental tests, the DMLS 17-4 PH compared with the rolled 17-4 PH stainless steel samples decreased the yield strength by ~8% and ultimate strength by ~11%. This mechanical behavior could be attributed to defects in the DMLS process, such as defects due to unfused voids and porosity [28,29]. The results provided by simulation fit with those from experimental analysis; this is due to

the integration of the experimental values (elastic modulus, tensile strength, yield strength of material, and the average experimental stress–strain curves) into the numerical model to predict the mechanical properties of the material and generating information about the mechanical properties of the materials. In this sense, the procedure followed by Zhang et al. [53] introduced the yielding and ultimate points into the numerical analysis by applying a minimal calibration to the strength coefficient and intrinsic strength term. A similar procedure was performed by Promsuwan et al. [52], where the numerical model is obtained from the strength coefficient and the strain hardening is obtained from the experimental procedure.

The SEM micrographs of fractography morphologies from the tensile fracture surface of rolled 17-4 PH and 17-4 PH DMLS stainless steel samples after tensile tests are shown in Figure 10. The fracture morphology of the surface of rolled 17-4 PH stainless steel presents the typical cone shape fracture as shown in Figure 11a,b. According to Figure 11b, large quantities of fine dimples characterize a ductile fracture mode. The fracture surface of 17-4 PH DMLS stainless steel samples showed elongated defects present in the fracture surfaces; they are associated with a partially fragile fracture mode and some defects due to unfused voids (see Figure 11c,d). On the other hand, the laser sintering caused strength and plasticity to decrease, which is exhibited in Figure 7b, causing the material to become brittle.

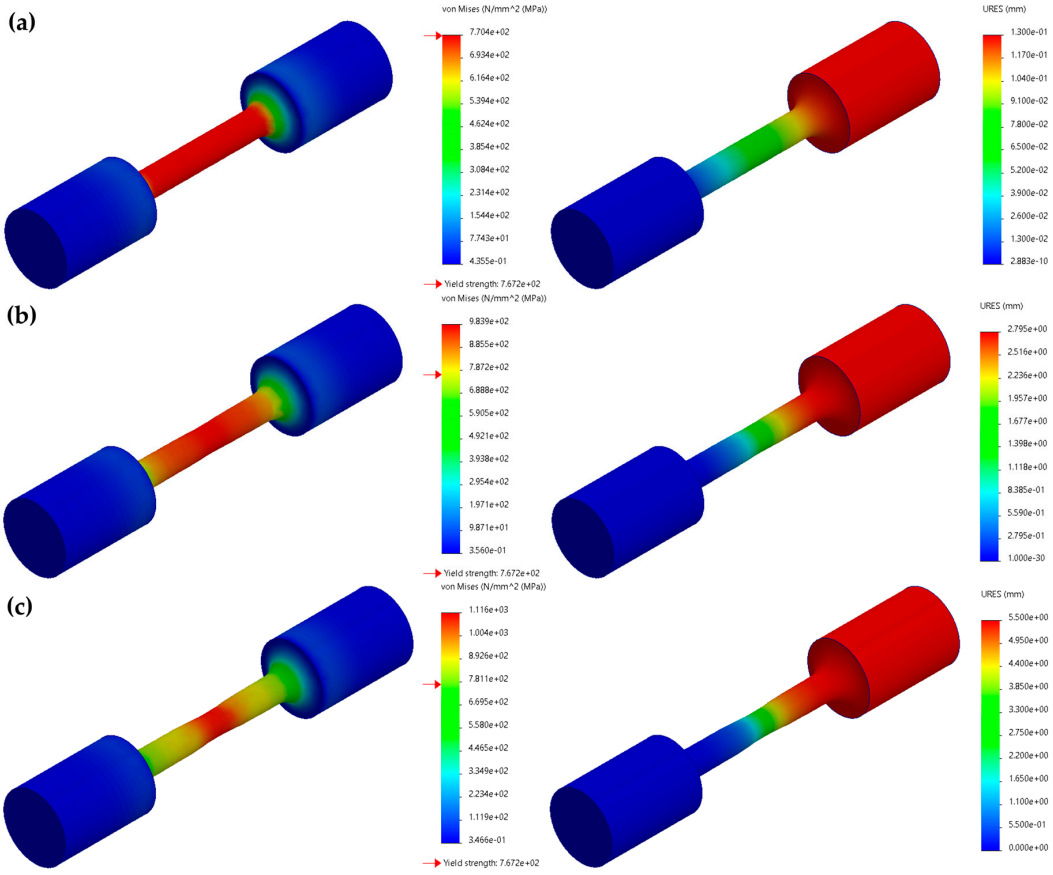

Figure 9. FEM simulation von Mises stress and axial displacement for rolled 17-4 PH at (**a**) yield strength, (**b**) ultimate strength, and (**c**) fracture strength.

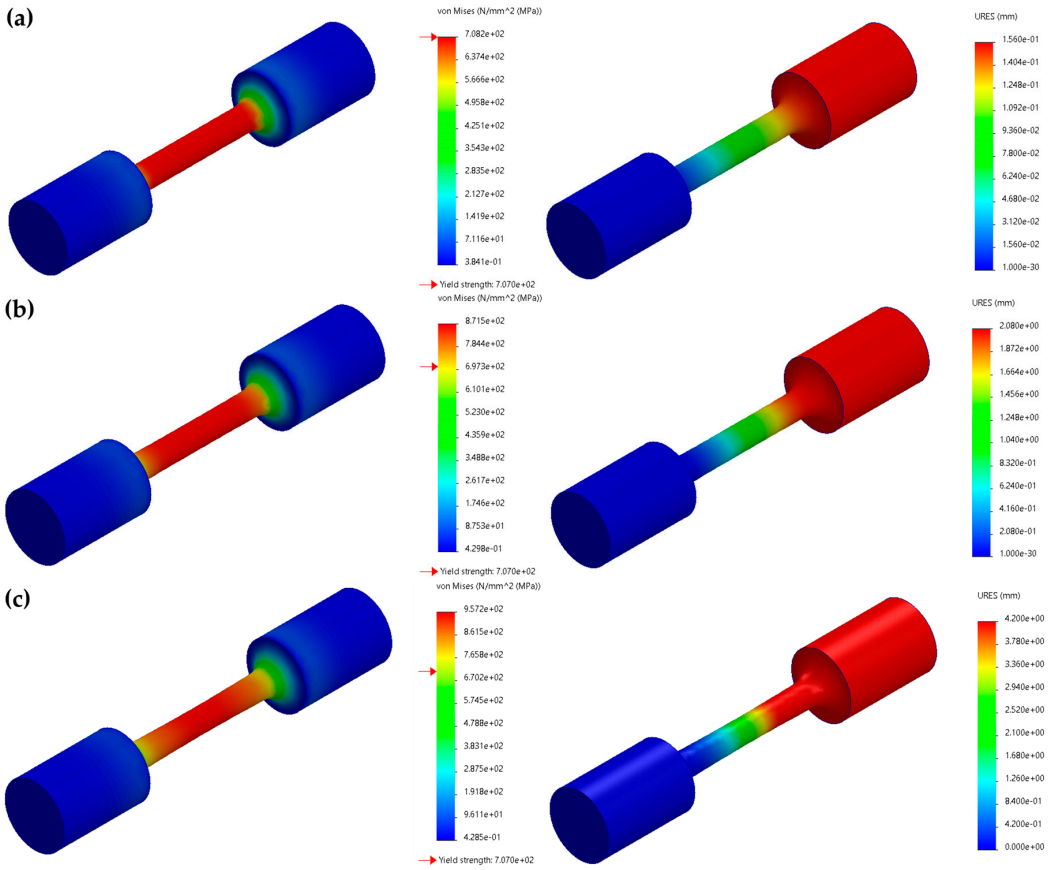

Figure 10. FEM simulation von Mises stress and axial displacement for 17-4 PH DMLS at (**a**) yield strength, (**b**) ultimate strength, and (**c**) fracture strength.

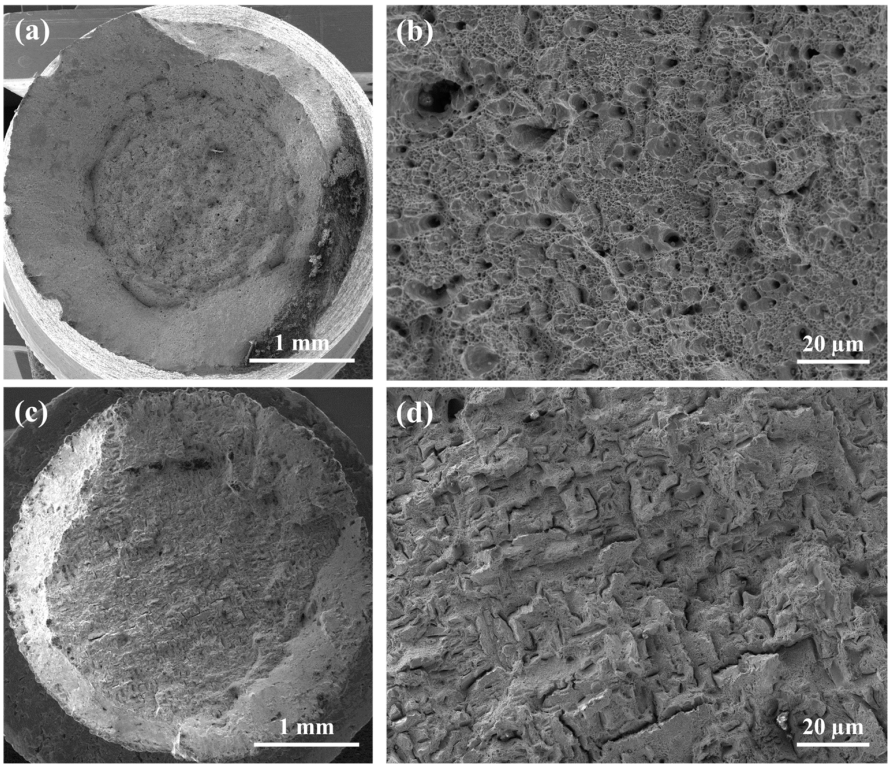

Figure 11. Fractography of tensile samples for (**a**,**b**) rolled 17-4 PH and (**c**,**d**) 17-4 PH DMLS.

5. Conclusions

This study analyzed the effect on the mechanical properties and microstructure of two manufacturing procedures—conventional machining and direct metal laser sintering—using experimental tensile tests and nanoindentation, as well as linear and nonlinear tensile finite element simulations. The study was conducted on commercial cold-rolled 17-4 PH and 17-4 PH stainless steel manufactured using direct metal laser sintering (DMLS). The findings are listed below:

- The rolled 17-4 PH stainless steel microstructure showed the typical martensitic structure for the longitudinal and transversal cross-sections. The microstructure for 17-4 PH DMLS stainless steel reveals the layers or levels of melting of the steel powder due to the laser process, characterized by complex directional columnar structures parallel to the DMLS build direction.
- Diffraction XRD patterns for rolled 17-4 PH stainless steel present ferritic (α) and austenitic (γ) phases. The XRD patterns for 17-4 PH DMLS stainless steel show the presence of both ferritic (α) or martensitic and austenitic (γ) phases.
- The mechanical properties obtained from the simple tension test decreased by 17% for the elastic modulus, 7.8% for the yield strength, and 7% ultimate strength for 17-4 PH DMLS compared with rolled 17-4 PH stainless steel.
- The nanoindentation results of mechanical properties analyzed for rolled 17-4 PH showed similar values for the longitudinal and transversal cross-sections. Meanwhile, the properties of 17-4 PH DMLS stainless steel samples presented an anisotropic behavior with a variation in the elastic modulus as result of the superposition of the DMLS layers.
- According to the experimental and simulated tests, the DMLS 17-4 PH compared with rolled 17-4 PH stainless steel samples decreased the yield strength by ~8% and the ultimate strength by ~11%. This mechanical behavior could be attributed to defects in the DMLS process, such as defects due to unfused voids and porosity.
- The fracture morphology of the surface of rolled 17-4 PH stainless steel presented the typical cone shape fracture, showing a ductile fracture mode that is characterized by the presence of large quantities of fine dimples. The fracture surface of 17-4 PH DMLS stainless steel samples showed elongated defects in the fracture surfaces associated with partially fragile fracture mode and some defects due to unfused voids. Also, the laser sintering process causes a decrease in strength and plasticity, resulting in the material's brittle behavior.

Author Contributions: Conceptualization, P.M.-G., M.A.-V. and R.C.-E.; methodology, J.A.B.-F., H.M.H.-G., J.C.D.-G. and R.M.-A.; software, M.A.-V.; validation, M.A.-V., P.M.-G. and R.C.-E.; formal analysis, M.A.-V., P.M.-G. and J.A.O.; investigation, P.M.-G.; resources, H.M.H.-G., J.C.D.-G., R.M.-A. and J.A.B.-F.; data curation, M.A.-V.; writing—original draft preparation, M.A.-V. and P.M.; writing—review and editing, J.A.O.; visualization, M.A.-V.; supervision, M.A.-V.; project administration, P.M.-G.; funding acquisition, R.C.-E. and M.A.-V. All authors have read and agreed to the published version of the manuscript.

Funding: The APC was funded by Universidad de las Américas Puebla.

Data Availability Statement: Data are included in the article. Additionally, data presented in this study are available in digital form on request from the corresponding author.

Acknowledgments: The authors would like to thank to Consejo Nacional de Humanidades Ciencias y Tecnologías, CONAHCYT, Mexico.

Conflicts of Interest: The authors declare no conflicts of interest.

References

1. Mirmahdi, E. Defects in Turbine Impeller Blades with Non-destructive Testing: Modeling, Ultrasonic Waves, Defect Analysis. *J. Inst. Eng. India Ser. C.* **2021**, *102*, 1395–1401. [CrossRef]
2. Yousefi, M.; Rajabi, M.; Yousefi, M.; Sadegh, M.; Kerahroodi, A. Failure Analysis of a 17-4 PH Stainless Steel Part in an Exhaust Fastener. *J. Fail. Anal. Prev.* **2021**, *21*, 2278–2289. [CrossRef]
3. Adamovic, D.; Ristic, B.; Zivic, F. Review of Existing Biomaterials-Method of Material Selection for Specific Applications in Orthopedics. In *Biomaterials in Clinical Practice*; Springer: Cham, Switzerland, 2018; pp. 47–99. [CrossRef]
4. Chan, Y.L.S.; Dlegel, O.; Xu, X. Bonding integrity of hybrid 18Ni300-17-4 PH steel using the laser powder bed fusion process for the fabrication of plastic injection mould inserts. *Int. J. Adv. Manuf. Technol.* **2022**, *120*, 4963–4976. [CrossRef]
5. Wang, Z.; Liu, Y.; Cheng, Q.; Xu, R.; Ma, Y.; Wu, D. Nonlinear sealing force of a seawater balance valve used in an 11,000-meter manned submersible. *Front. Mech. Eng.* **2023**, *18*, 10. [CrossRef]
6. Vunnam, S.; Saboo, A.; Sudbrack, C.; Starr, T. Effect of powder chemical composition on the as-built microstructure of 17-4 PH stainless steel processed by selective laser melting. *Addit. Manuf.* **2019**, *30*, 100876. [CrossRef]
7. Wang, D.; Chi, C.T.; Wang, W.Q.; Li, Y.L.; Wang, M.S.; Chen, X.G.; Chen, Z.H.; Cheng, X.P.; Xie, Y.J. The effects of fabrication atmosphere condition on the microstructural and mechanical properties of laser direct manufactured stainless steel 17-4 PH. *J. Mater. Sci. Technol.* **2019**, *35*, 1315–1322. [CrossRef]
8. Sabooni, S.; Chabok, A.; Feng, S.C.; Blaauw, H.; Pijper, T.C.; Yang, H.J.; Pei, Y.T. Laser powder bed fusion of 17–4 PH stainless steel: A comparative study on the effect of heat treatment on the microstructure evolution and mechanical properties. *Addit. Manuf.* **2021**, *46*, 102176. [CrossRef]
9. Carneiro, L.; Jalalahmadi, B.; Ashtekar, A.; Jiang, Y. Cyclic deformation and fatigue behavior of additively manufactured 17–4PH stainless steel. *Int. J. Fatigue* **2019**, *123*, 22–30. [CrossRef]
10. Ara, I.; Eshkabilov, S.; Azarmi, F.; Sevostianov, I.; Tangpong, X.W. Investigation on elastic properties and unconventional plasticity of 316L stainless steel processed by selective laser melting technology. *Prog. Addit. Manuf.* **2022**, *7*, 1169–1181. [CrossRef]
11. Luecke, W.E.; Slotwinski, J.A. Mechanical Properties of Austenitic Stainless Steel Made by Additive Manufacturing. *J. Res. Natl. Inst. Stand. Technol.* **2014**, *119*, 398–418. [CrossRef]
12. Yeon, S.M.; Yoon, J.; Kim, T.B.; Lee, S.H.; Jun, T.S.; Son, Y.; Choi, K. Normalizing Effect of Heat Treatment Processing on 17-4 PH Stainless Steel Manufactured by Powder Bed Fusion. *Metals* **2022**, *12*, 704. [CrossRef]
13. KC, S.; Nezhadfar, P.D.; Phillips, C.; Kennedy, M.S.; Shamsaei, N.; Jackson, R.L. Tribological behavior of 17–4PH stainless steel fabricated by traditional manufacturing and laser-based additive manufacturing methods. *Wear* **2019**, *440–441*, 203100. [CrossRef]
14. Muslim, T.; Karagoz, T.; Kurama, S.; Sezer, P.; Yazici, O.F.; Ozkok, R. Laser metal deposition of 17–4 PH stainless steel: Geometrical, microstructural, and mechanical properties investigation for structural applications. *CIRP J. Manuf. Sci. Technol.* **2023**, *41*, 69–79. [CrossRef]
15. Rehman, F.; Cashell, K.A.; Anguilano, L. Post-fire Structural Properties of Hot-Rolled and Cold-Rolled Duplex Stainless Steel Reinforcing Bar. *Fire Technol.* **2022**, *58*, 2283–2311. [CrossRef]
16. Li, D.; Xu, L.; Li, L.; Yue, C.; Zhou, W.; Zhang, C. Finite element simulation for straightedge lineal roll forming process of high frequency welding pipe. *Int. Interact. Des. Manuf.* **2023**, *17*, 1–9. [CrossRef]
17. Mohanty, I.; Das, P.; Bhattacharjee, D.; Datta, S. In Search of the Attributes Responsible for Sliver Formation in Cold Rolled Steel Sheets. *J. Inst. Eng. India Ser. D.* **2017**, *98*, 59–70. [CrossRef]
18. Sheng, L.I.; Na, L.I.; Xing, P.; Xiang, L.U.; Ji, L.I. Fatigue Property of Hot Rolled and Cold Rolled Strips. *J. Iron Steel Res. Int.* **2013**, *20*, 48–51.
19. Agrawal, P.; Aggarwal, S.; Banthia, N.; Singh, U.S.; Kalia, A.; Pesin, A. A comprehensive review on incremental deformation in rolling processes. *J. Eng. Appl. Sci.* **2022**, *69*, 20. [CrossRef]
20. Mohammadzehi, S.; Mirzadeh, H. Cold unidirectional/cross-rolling of austenitic stainless steels: A review. *Arch. Civ. Mech.* **2022**, *22*, 129. [CrossRef]
21. Ikumapayi, O.M.; Akinlabi, E.T.; Onu, P.; Abolusoro, O.P. Rolling operation in metal forming: Process and principles—A brief study. *Mater. Today Proc.* **2020**, *26*, 1644–1649. [CrossRef]
22. Guo, N.; Leu, M.C. Additive manufacturing: Technology, applications and research needs. *Front. Mech. Eng.* **2013**, *8*, 215–243. [CrossRef]
23. Spoward, J.E.; Gupta, N.; Lehmhus, D. Additive Manufacturing of Composites and Complex Materials. *JOM* **2018**, *70*, 272–274. [CrossRef]
24. Everton, S.K.; Hirsch, M.; Stravroulakis, P.; Leach, R.K.; Clare, A.T. Review of in-situ process monitoring and in-situ metrology for metal additive manufacturing. *Mater. Des.* **2016**, *95*, 431–445. [CrossRef]
25. Chauhan, A.K.S.; Shukla, M.; Kumar, A. 3D thermal simulation of powder bed fusion additive manufacturing of stainless steel. *Int. J. Interact. Des. Manuf.* **2023**, *17*, 517–524. [CrossRef]
26. Wu, Z.; Basu, D.; Meyer, J.L.L.; Larson, E.; Kuo, R.; Beuth, J.; Rollett, A. Study of Powder Gas Entrapment and Its Effects on Porosity in 17-4 PH Stainless Steel Parts Fabricated in Laser Powder Bed Fusion. *JOM* **2021**, *73*, 177–188. [CrossRef]
27. Sghaier, T.A.M.; Sahlaoui, H.; Mabrouki, T.; Sallem, H.; Rech, J. Selective Laser Melting of Stainless-Steel: A Review of Process, Microstructure, Mechanical Properties and Post-Processing treatments. *Int. J. Mater. Form.* **2023**, *16*, 41. [CrossRef]

28. Gatões, D.; Alves, R.; Alves, B.; Vieira, M.T. Selective Laser Melting and Mechanical Properties of Stainless Steels. *Materials* **2022**, *15*, 7575. [CrossRef]
29. Zhao, Z.; Zhang, L.; Du, W.; Bai, P.; Li, J.; Zhang, W.; Yuan, X. Microstructure and Properties of Porous 17-4 PH Stainless Steel Prepared by Selective Laser Melting. *Trans. Indian. Inst. Met.* **2022**, *75*, 1641–1648. [CrossRef]
30. Nezhadfar, P.D.; Gradl, P.R.; Shao, S.; Shamsaei, N. Microstructure and Deformation Behavior of Additively Manufactured 17–4 Stainless Steel: Laser Powder Bed Fusion vs. Laser Powder Directed Energy Deposition. *JOM* **2022**, *74*, 1136–1148. [CrossRef]
31. Akessa, A.D.; Tucho, W.M.; Lemu, H.G.; Grønsund, J. Investigations of the Microstructure and Mechanical Properties of 17-4 PH ss Printed Using a MarkForged Metal, X. *Materials* **2022**, *15*, 6898. [CrossRef]
32. Rafi, H.K.; Pal, D.; Patil, N.; Starr, T.L.; Stucker, B.E. Microstructure and Mechanical Behavior of 17-4 Precipitation Hardenable Steel Processed by Selective Laser Melting. *J. Mater. Eng. Perform.* **2014**, *23*, 4421–4428. [CrossRef]
33. Henry, T.C.; Morales, M.A.; Cole, D.P.; Shumeyko, C.M.; Riddick, J.C. Mechanical Behavior of 17-4 PH stainless steel processed by atomic diffusion additive manufacturing. *Int. J. Adv. Manuf. Technol.* **2021**, *114*, 2103–2114. [CrossRef]
34. Yadollahi, A.; Shamsaei, N.; Thompson, S.M.; Elwany, A.; Bian, L. Mechanical and microstructural properties of selective laser melted 17-4 PH stainless steel. In Proceedings of the ASME international mechanical engineering congress and exposition. American Society of Mechanical Engineers, Houston, TX, USA, 13–19 November 2015; pp. 1–7.
35. Tolosa, I.; Garciandía, F.; Zubiri, F.; Zapirain, F.; Esnaola, A. Study of mechanical properties of AISI 316 stainless steel processed by "selective laser melting", following different manufacturing strategies. *Int. J. Adv. Manuf. Technol.* **2010**, *51*, 639–647. [CrossRef]
36. Suwanpreecha, C.; Seensattayawong, P.; Vadhanakovint, V.; Manonukul, A. Influence of Specimen Layout on 17-4 PH (AISI 630) Alloys Fabricated by Low-Cost Additive Manufacturing. *Metall. Mater. Trans. A Phys.* **2021**, *52*, 1999–2009. [CrossRef]
37. Kedziora, S.; Decker, T.; Museyibov, E.; Morbach, J.; Hohmann, S.; Huwer, A.; Wahl, M. Strength Properties of 316L and 17-4 PH Stainless Steel Produced with Additive Manufacturing. *Materials* **2022**, *15*, 6278. [CrossRef] [PubMed]
38. Mahmoudi, M.; Elwany, A.; Yadollahi, A.; Thompson, S.M.; Bian, L.; Shamsaei, N. Mechanical properties and microstructural characterization of selective laser melted17-4 PH stainless steel. *Rapid Prototyp. J.* **2017**, *23*, 280–294. [CrossRef]
39. Alkindi, T.; Alyammahi, M.; Susantyoko, R.A.; Atatreh, S. The effect of varying specimens' printing angles to the bed surface on the tensile strength of 3D-printed 17-4 PH stainless-steels via metal FFF additive manufacturing. *MRS Commun.* **2021**, *11*, 310–316. [CrossRef]
40. Malakshah, M.G.; Eslami, A.; Ashrafizadeh, F.; Berenjkoub, A. Effect of Heat Treatment on Corrosion, Fatigue, and Corrosion Fatigue Behavior of 17-4 PH Stainless Steel. *J. Mater. Eng. Perform.* **2023**, *32*, 6610–6621. [CrossRef]
41. Nezhadfar, P.D.; Shrestha, R.; Phan, N.; Shamsaei, N. Fatigue behavior of additively manufactured 17-4 PH stainless steel: Synergistic effects of surface roughness and heat treatment. *Int. J. Fatigue* **2019**, *124*, 188–204. [CrossRef]
42. Huber, D.; Vogel, L.; Fischer, A. The effects of sintering temperature and hold time on densification, mechanical properties and microstructural characteristics of binder jet 3D printed 17-4 PH stainless steel. *Addit. Manuf.* **2021**, *46*, 102114. [CrossRef]
43. Wilcox, H.; Lewis, B.; Styman, P. Evaluation of the Mechanical Properties of Precipitation-Hardened Martensitic Steel 17-4 PH using Small and Shear Punch Testing. *J. Mater. Eng. Perform.* **2021**, *30*, 4206–4216. [CrossRef]
44. Qin, F.; Shi, Q.; Zhou, G.; Liu, X.; Chen, L.; Du, W.; Yao, D. Influence of powder particle size distribution on microstructure and mechanical properties of 17-4 PH stainless steel fabricated by selective laser Melting. *J. Mater. Res. Technol.* **2023**, *25*, 231–240. [CrossRef]
45. Wu, M.; Huang, Z.; Tseng, C.; Hwang, K. Microstructures, Mechanical Properties, and Fracture Behaviors of Metal-Injection Molded 17-4 PH Stainless Steel. *Met. Mater. Int.* **2015**, *21*, 531–537. [CrossRef]
46. Auguste, P.; Mauduit, A.; Fouquet, L.; Pillot, S. Study on 17-4 PH stainless steel produced by selective laser melting. *Sci. Bull. B Chem. Mater. Sci. UPB* **2018**, *80*, 197–210.
47. El Moghazi, S.N.; Wolfe, T.; Ivey, D.G.; Henein, H. Plasma transfer arc additive manufacturing of 17-4 PH: Assessment of defects. *Int. J. Adv. Manuf. Technol.* **2020**, *108*, 2301–2313. [CrossRef]
48. Sarma, I.K.; Selvaraj, N.; Kumar, A. Parametric investigation and characterization of 17-4 PH stainless steel parts fabricated by selective laser melting. *J. Cent. South. Univ.* **2023**, *30*, 855–870. [CrossRef]
49. Kartikeya, I.; Selvraj, N.; Kumar, A. A Review on Microstructure and Mechanical Properties of L-PBF 17-4 PH and 15-5PH SS. In *Recent Advances in Manufacturing Processes and Systems*; Springer: Singapore, 2022; pp. 37–53. [CrossRef]
50. Song, B.; Zhao, X.; Li, S.; Han, C.; Wei, Q.; Wen, S.; Liu, J.; Shi, Y. Differences in microstructure and properties between selective laser melting and traditional manufacturing for fabrication of metal parts: A review. *Front. Mech. Eng.* **2015**, *10*, 111–125. [CrossRef]
51. Porro, M.; Zhang, B.; Parmar, A.; Shin, Y. Data Driven Modeling of Mechanical Properties for 17 4 PH Stainless Steel Built by Additive Manufacturing. *Integr. Mater. Manuf. Innov.* **2022**, *11*, 241–255. [CrossRef]
52. Promsuwan, P.; Tongsri, R.; Kowitwarangkul, P.; Ninpetch, P.; Threrujirapapong, T. Investigation on microstructure and mechanical properties of 17-4 PH stainless steels fabricated by materials extrusion additive manufacturing. *Songklanakarin J. Sci. Technol.* **2023**, *45*, 442–450.
53. Zhang, Q.; Wie, J.; London, T.; Griffiths, D.; Bhamji, I.; Oancea, V. Estimates of the mechanical properties of laser powder bed fusion Ti-6Al-4V parts using finite element models. *Mater. Des.* **2019**, *169*, 107678. [CrossRef]
54. *ASTM A370-03a*; Standard Test Methods and Definitions for Mechanical Testing of Steel Products. ASTM: West Conshohocken, PN, USA, 2017.

55. Leo, P.; D'Ostuni, S.; Perulli, P.; Sastre, M.A.C.; Fernández-Abia, A.I.; Barreiro, J. Analysis of microstructure and defects in 17-4 PH stainless steel sample manufactured by Selective Laser Melting. *Procedia Manuf.* **2019**, *41*, 66–73. [CrossRef]
56. Aripin, M.A.; Sajuri, Z.; Jamadon, N.H.; Baghdadi, A.H.; Syarif, J.; Mohamed, I.F.; Aziz, A.M. Effects of Build Orientations on Microstructure Evolution, Porosity Formation, and Mechanical Performance of Selective Laser Melted 17-4 PH Stainless Steel. *Metals* **2022**, *12*, 1968. [CrossRef]
57. Fischer-Cripps, A.C. *Nanoindentation*, 3rd ed.; Springer: New York, NY, USA, 2011.
58. Mazeran, P.-E.; Beyaoui, M.; Bigerelle, M.; Guigon, M. Determination of mechanical properties by nanoindentation in the case of viscous materials. *Int. J. Mater. Res.* **2012**, *103*, 715–722. [CrossRef]
59. Espitia, L.A.; Dong, H.; Li, X.-Y.; Pindeo, C.E.; Tschiptschin, P.A. Scratch test of active screen low temperature plasma nitrided AISI 410 martensitic stainless steel. *Wear* **2017**, *376–377*, 30–36. [CrossRef]
60. Alfieri, V.; Giannella, V.; Caiazzo, F.; Sepe, R. Influence of position and building orientation on the static properties of LPBF specimens in 17-4 PH stainless steel. *Forces Mech.* **2022**, *8*, 100–108. [CrossRef]

Disclaimer/Publisher's Note: The statements, opinions and data contained in all publications are solely those of the individual author(s) and contributor(s) and not of MDPI and/or the editor(s). MDPI and/or the editor(s) disclaim responsibility for any injury to people or property resulting from any ideas, methods, instructions or products referred to in the content.